DOI: 10.1143/JPSJ.80.023710

Propeller-Like Low Temperature Fermi Surface of $Ba_{1-x}K_xFe_2As_2$ from Magnetotransport and Photoemission Measurements

Daniil V. EVTUSHINSKY[1], Alexander A. KORDYUK[1,2], Volodymyr B. ZABOLOTNYY[1], Dmytro S. INOSOV[3], Timur K. KIM[1], Bernd BÜCHNER[1], Huiqian LUO[4], Zhaosheng WANG[4], Hai-Hu WEN[4], Guoli SUN[3], Chengtian LIN[3], and Sergey V. BORISENKO[1]

[1]*Institute for Solid State Research, IFW Dresden, P. O. Box 270116, D-01171 Dresden, Germany*
[2]*Institute of Metal Physics of National Academy of Sciences of Ukraine, 03142 Kyiv, Ukraine*
[3]*Max-Planck-Institute for Solid State Research, Heisenbergstrasse 1, D-70569 Stuttgart, Germany*
[4]*Institute of Physics, Chinese Academy of Sciences, Beijing 100190, China*

(Received August 31, 2010; accepted December 14, 2010; published online February 10, 2011)

The Hall coefficient of the hole-doped iron arsenide $Ba_{1-x}K_xFe_2As_2$ (BKFA) is calculated purely on the basis of the electronic structure, revealed in the angle-resolved photoemission spectroscopy (ARPES) experiments, and compared to the one measured directly. The observed agreement allows us to state that upon cooling the Fermi surface (FS) in the optimally doped BKFA gradually evolves to the propeller-like topology, on which the superconductivity develops. Persistence of the notable temperature dependence in both photoemission and magnetotransport experiments well above the spin-density-wave (SDW) transition suggests that the FS reconstruction in BKFA is partially decoupled from the emergence of static magnetism.

KEYWORDS: photoemission, iron arsenides, Hall effect, electrical transport, resistivity, band structure, superconductivity

The discovery of iron-based high temperature superconductors faced theoreticians and experimentalists with numerous questions concerning the electronic structure of newly emerged materials. The low energy electronic band dispersion, and in particular the shape of the Fermi surface (FS), are decisive properties of any superconductor, as they are forming premises for theoretical description of the superconductivity.[1)] Naturally, the issue of the FS geometry of iron-arsenide high-T_c family was addressed in many theoretical[2–4)] and experimental[5–13)] studies. Primarily the FS was assumed to consist of two hole-like sheets around the center of FeAs Brillouin zone and two electron-like sheets at the corners. Contrary to this assumption, some angle-resolved photoemission spectroscopy (ARPES) studies have suggested a notable difference in the topology of the low temperature FS — namely a shallow propeller-like structure has been detected at the corners of the Brillouin zone, X point [see Fig. 1(a), and refs. 5–9]. However, the vast majority of experimental studies on these materials still adhere to the early ideas of the FS shape in the interpretation of their results; similarly, most of theoretical studies still use such FS as a starting basis. Below by means of combined ARPES and Hall measurements we show that the propeller-like FS topology is a robust inherent bulk property of the optimally doped $Ba_{1-x}K_xFe_2As_2$ (BKFA). Furthermore, temperature trend of the photoemission and transport signals suggests that the FS reconstruction in BKFA is partially decoupled from the formation of the static spin-density-wave (SDW).

The Hall coefficient (R_H), calculated purely on the basis of the band dispersion, extracted from the ARPES spectra of BKFA, was compared to the direct magnetotransport measurements. The demonstrated agreement implies that the FS of BKFA changes gradually with temperature, and the superconductivity develops on the propeller-like FS. At the same time it becomes clear that the band structure, calculated without any additional order, fails to explain temperature-dependent transport measurements in iron arsenides, and is capable to describe only high temperature properties.

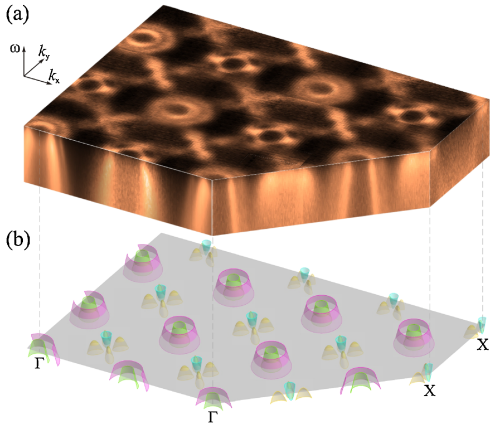

Fig. 1. (Color online) (a) Three-dimensional sketch of low temperature $Ba_{1-x}K_xFe_2As_2$ ARPES data, shown for the energy range of approximately −50 to 0 meV. (b) Band dispersion, extracted from fitting of ARPES spectra,[22)] shown for the energy range of −20 to 20 meV.

Resistivity and Hall effect measurements were carried out on self-flux-grown single crystals of BKFA with $T_c = 36$, 30, 25, 23 K and doping levels $x = 0.40$, 0.284, 0.235, 0.22, respectively[14)] in the National Laboratory for Superconductivity, Institute of Physics, Beijing. Photoemission experiments were carried out on Sn-flux-grown single crystals of BKFA with $T_c = 32$ K and doping level $x = 0.32$,[15,16)] and later confirmed by measurements of the self-flux-grown single crystals at the 1^3-ARPES[17)] end station at BESSY synchrotron in Berlin (Helmholtz-Zentrum für Materialien und Energie).

For quasi two-dimensional materials[18)] the in-plane conductivity tensor,

$$\sigma = \begin{pmatrix} \sigma_{xx} + \delta\sigma_{xx} & \sigma_{xy} \\ -\sigma_{xy} & \sigma_{xx} + \delta\sigma_{xx} \end{pmatrix}, \quad (1)$$

in the presence of external magnetic field, directed along the c axis, B, can be expressed up to terms in B^2 through the integrals over the FS in the following way:[19,20)]

Table I. Average v_F and ρ_F with approximate error bars, as well as relative contributions to σ_{xx}, σ_{xy}, and $\delta\sigma_{xx}$ for different FS sheets, as derived from low temperature ARPES measurements on $Ba_{1-x}K_xFe_2As_2$ ($x = 0.32$).

	$\langle v_F \rangle$ (eV Å)	$\langle \rho_F \rangle$ (Å^{-1})	σ_{xx}	σ_{xy}	$\delta\sigma_{xx}$
Inner Γ-barrel	0.52 ± 0.05	0.14 ± 0.01	0.27	0.84	−0.17
Outer Γ-barrel	0.40 ± 0.04	0.30 ± 0.04	0.45	0.49	−0.04
X-pocket	$0.57^{+0.00}_{-0.20}$	0.06 ± 0.02	0.13	−1.0	−0.51
Blades	0.33 ± 0.10	0.06 ± 0.02	0.28	1.42	−0.56

$$\sigma_{xx} = \frac{\tau e^2}{2\pi L_c h} \int v_F(\mathbf{k})\, dk, \tag{2}$$

$$\sigma_{xy} = \frac{\tau^2 B e^3}{L_c h^2} \int \frac{v_F^2(\mathbf{k})}{\rho_F(\mathbf{k})}\, dk, \tag{3}$$

$$\delta\sigma_{xx} = -\frac{4\pi\tau^3 B^2 e^4}{L_c h^3} \int \left\{ v_F(\mathbf{k}) \left[\frac{dv_F(\mathbf{k})}{dk} \right]^2 + \frac{v_F^3(\mathbf{k})}{2\rho_F^2(\mathbf{k})} \right\} dk, \tag{4}$$

where $\mathbf{k}$ is the quasimomentum, v_F is the Fermi velocity, ρ_F[21] is the FS curvature radius (note that it is the only quantity in these formulas that can be negative), dk is the element of the FS length, τ is the quasiparticle lifetime in the vicinity of the Fermi level (hereafter assumed to be $\mathbf{k}$-independent), L_c is the size of the primitive elementary cell along the c-axis, h is the Plank's constant, and e is the elementary charge.

The band dispersion, which is the input parameter to calculate σ with eqs. (2)–(4), was extracted from the fit of BKFA ARPES spectra, taken below and above T_c.[22] The overview of the low-temperature ARPES data and extracted band dispersion are presented in Fig. 1. Average v_F and ρ_F, as well as contributions from different FS sheets to the components of the conductivity tensor at the temperature just above T_c are summarized in Table I. We stress that the propeller-like structure at the corner of the Brillouin zone develops steadily upon cooling, is not related to the opening of the superconductinging gap, and is present above the temperature of magnetic transition, $T_{SDW} = 70\,K$[16] (Fig. 2).

The quantities, which are usually measured experimentally, resistivity, Hall coefficient, and magnetoresistivity, can be expressed in terms of σ:

$$\rho = \frac{1}{\sigma_{xx}}, \quad R_H = \frac{\sigma_{xy}}{B \cdot \sigma_{xx}^2}, \quad \frac{\delta\rho}{\rho} = -\frac{\delta\sigma_{xx}}{\sigma_{xx}} - \frac{\sigma_{xy}^2}{\sigma_{xx}^2}. \tag{5}$$

Hall effect is one of the few tangible properties of a crystalline solid, which can distinguish between electron- and hole-like nature of the FS. Figure 3(a) shows the comparison of the Hall coefficient of nearly optimally doped BKFA, calculated from the electronic band structure, to the directly measured one. The measured R_H exhibits *gradual* variation over entire temperature range — smoothly starts to increase already from room temperature, and shows no abrupt changes at the SDW transition. Such temperature dependence of R_H is inline with the temperature trend of photoemission spectra (Fig. 2), indicating a *gradual* evolution of the FS to the propeller-like topology with cooling. In the calculation the high temperature point corresponds to the

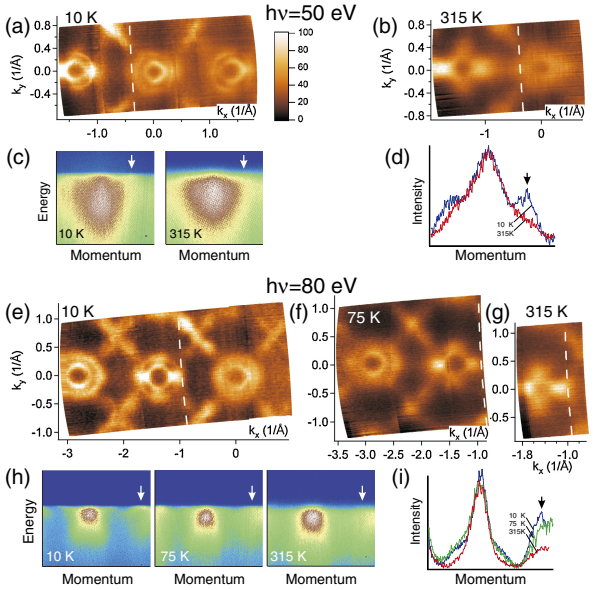

Fig. 2. (Color online) Temperature evolution of the $Ba_{1-x}K_xFe_2As_2$ ($x = 0.32$) Fermi surface (FS), seen in ARPES: the propeller-like structure at the corner of the Brillouin zone emerges gradually upon cooling. (a, b) FS, imaged with 50 eV excitation energy at 10 and 315 K keeping other experimental conditions the same. (c) Two equivalent energy-momentum cuts, indicated by white dashed lines in the panels (a) and (b). (d) Corresponding momentum distribution curves (MDC), integrated around the Fermi level. (e, f, g) FS, imaged with 80 eV excitation energy at 10, 75, and 315 K in same experimental conditions. (h) Cuts, indicated in the panels (e, f, g). (i) Corresponding MDC at the Fermi level. Arrows in panels (c, d, h, i) indicate the intensity, corresponding to the blades.

FS, obtained theoretically without any additional ordering,[23] while the low temperature point corresponds to the band dispersion, extracted from ARPES spectra.[22] Agreement between measured and calculated R_H suggests that high temperature FS indeed resembles the one obtained in theoretical calculations (somewhat larger measured value is consistent with remnants of the FS reconstruction even at room temperature), while the strong increase of R_H at low temperatures originates from the reconstruction of the FS into the propeller-like topology seen by ARPES.

Following remark is appropriate here. We have succeeded to describe the Hall coefficient of BKFA, both the absolute value and the variation with temperature, within the isotropic scattering rate approximation; it is known that such approximation holds for many different compounds, e.g., it was checked for simple metals and transition metal dichalcogenides.[19,24] Though the temperature-dependent R_H may result from the lifetime variations over the FS without any changes in the FS contours[25–27] (in this case the anisotropy of the lifetime is usually used as a fitting parameter), such scenario seem to be incapable of explaining the Hall coefficient behavior in ferropnictides. The variation of the scattering rate between hole- and electron-like bands cannot account for huge changes in R_H of the parent compound — even assuming the lifetime infinitely larger for the hole carriers than for electron ones or *vice versa*, we arrive at $|R_H| = 2.7 \times 10^{-9}\,m^3/C$, a value 10 times less than the measured one [see Fig. 3(c) and data in the refs. 28–30]. At the same time the mentioned FS reconstruction may be able to explain temperature dependence of the Hall effect for the entire phase diagram.

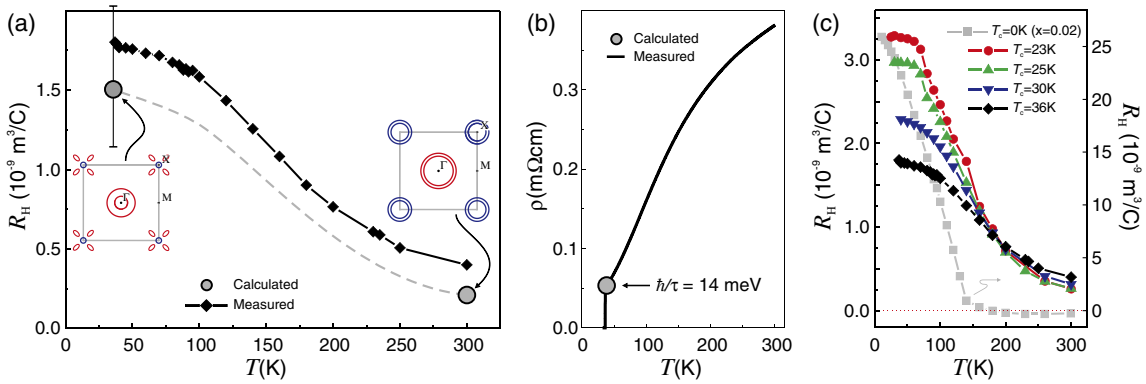

Fig. 3. (Color online) (a) The Hall coefficient (R_H) for nearly optimally doped $Ba_{1-x}K_xFe_2As_2$ as calculated on the basis of the band structure and as measured experimentally ($T_c = 36$ K). Insets show the high and low temperature FSs for $Ba_{1-x}K_xFe_2As_2$. The comparison of the measured and calculated R_H suggests that FS of $Ba_{1-x}K_xFe_2As_2$ evolves from the theoretically predicted at high temperatures to the one observed in low temperature ARPES measurements. (b) The temperature dependence of the in-plane resistivity for the same material. Knowledge of the band structure and electrical resistivity allows us to find that the scattering rate just above T_c equals 14 meV. (c) Temperature dependence of R_H for $Ba_{1-x}K_xFe_2As_2$ with different doping levels, and critical temperatures as indicated in the legend.

Leaving aside the complicated case of low doping levels with large SDW order parameter, we go to the relatively simple overdoped material on the electron side of the phase diagram, $BaFe_{2-x}Co_xAs_2$ (BFCA). For heavily overdoped BFCA the Hall effect is nearly temperature independent with $R_H \simeq (-1 \text{ to } -2.5) \times 10^{-9}$ m^3/C,[28,29] while the calculation from ARPES yields $R_H \simeq -2 \times 10^{-9}$ m^3/C (extraction of the band dispersion from photoemission spectra of BFCA will be presented elsewhere), providing another evidence for validity of the formulas (2)–(4) in the case of ferropnictides.[31] Similarly, good agreement between calculated from ARPES and measured parameters was found in the case of LiFeAs.[32,33] It is also important to note that for the mentioned overdoped BFCA and stoichiometric LiFeAs the Fermi surface indeed consists of hole-like sheets around Γ point and electron-like sheets around the corner of FeAs Brilloiun zone,[34] i.e. is close to the obtained in the band structure calculations, as well as it is in the case of some other iron arsenides.[35] Fermi surface shape and sign of the Hall effect for some iron arsenides is collected in the Table II.

Similarly to the expression for R_H, τ cancels out from the expression $\rho^2 \cdot \delta\rho/(\rho \cdot B^2)$ [see eqs. (2), (4), (5)], which means that this relation is also defined purely by the band dispersion. The reconstruction of the electronic structure results in a strong variation of this quantity. In the case of BKFA the low temperature value of $\rho^2 \cdot \delta\rho/(\rho \cdot B^2)$, calculated for the propeller-like FS, is 20–60 times larger than the value, calculated for high-temperature theoretical FS. Note that the magnetoresistivity is determined by the small FS sheets (see Table I), and therefore the uncertainty in the calculated value is quite large.

The value of the quasiparticle lifetime near the Fermi level affects measured signal in different types of experiments — for instance, the electrical conductivity is proportional to τ, and in ARPES τ results in the spectral line broadening. Since experimental resolution also leads to the broadening of photoemission lines (especially nasty in this sense is momentum resolution, which may vary from sample to sample, and is hard to determine), the analysis of the spectral widths only allows putting the upper limit on the scattering rate ($\hbar/\tau$),[36] which in the present case is of the order of 20 meV for $T \gtrsim T_c$. A more precise estimate for τ can be derived from combined knowledge of electrical conductivity and the band dispersion near the Fermi level by utilizing eq. (2), which basically says that the electrical conductivity is proportional to the lifetime multiplied by the Fermi surface perimeter and the Fermi velocity. In our case the combination of transport measurements of conductivity and ARPES measurements of the band dispersion yields $\tau = 5 \times 10^{-14}$ s ($\hbar/\tau = 14$ meV) for $T \gtrsim T_c$ [Fig. 3(b)]. Interestingly, the scattering rate in the superconducting state can be estimated from spectroscopic data as the width of the coherence peak, which is independent of the momentum resolution. For BKFA such estimate at $T \lesssim 10$ K yields a scattering rate of 1–2 meV.[37,38] The values of τ, obtained here from spectroscopic and transport data agree well with surface impedance measurements.[39]

Table II. (Color online) Form of the Fermi surface of some iron arsenide superconductors at the corner of the FeAs Brillouin zone (BZ)[8,34,35] and the sign of the Hall coefficient.[28,29,33] The electron-like bands at the BZ corner possess smaller effective band mass than the hole-like bands in the BZ center, and thus contribute more to the electronic transport (if form comparable FS sheets), implying negative R_H even for zero carrier doping.

Compound	FS sheets at the corner of BZ	Sign of R_H
$Ba_{1-x}K_xFe_2As_2$	(4 hole-like, 1 electron-like)	+
KFe_2As_2	(4 hole-like)	?
$BaFe_{2-x}Co_xAs_2$	(2 electron-like)	−
LiFeAs	(2 electron-like)	−
$BaFe_2As_{2-x}P_x$	(2 electron-like)	−

Above we have shown that the temperature-dependent ARPES (Fig. 2) and Hall data (Fig. 3), measured on BKFA, consistently point to the reconstruction of the FS to the propeller-like topology at low temperatures. What could be the reason for such modification of the electronic structure? Natural candidate is fluctuations of the SDW order: first, generally (π, π) magnetic interaction is well known to be strong and important in the iron arsenides, and second, temperature dependencies of the photoemission and magnetotransport data resemble those of the antiferromagnetic

fluctuations, detected by nuclear magnetic resonance (NMR) measurements of BKFA.[40] Similar correlation between the onset of antiferromagnetic correlations and the variation of the Hall coefficient was recently observed in $BaFe_2As_{2-x}P_x$.[41,42] Detailed search for the corresponding changes in the electronic structure of this material is still to be performed.

In conclusion, we have found that both magnetotransport and photoemission measurements are consistent with the steady evolution of the FS of the optimally doped $Ba_{1-x}K_xFe_2As_2$ to the propeller-like topology at low temperatures. The temperature trend of ARPES (Fig. 2) and Hall [Fig. 3(a)] signals imply presence of the FS reconstruction well above T_{SDW} (similar to the reported persistence of ordering signatures in cuprates[43] and dichalcogenides[44]), which in turn suggests that in $Ba_{1-x}K_xFe_2As_2$ the band reconstruction is partially decoupled from the static SDW. For lower doping levels the temperature variation of the Hall coefficient becomes much stronger [Fig. 3(c), refs. 28–30], which unambiguously points to a more prominent band reconstruction in the underdoped samples — most probably, the entire FS breaks into small pockets, though detailed picture in this case is still to be drawn.

Acknowledgments The work done in Dresden is a part of the FOR538 and was supported by the DFG under Grants No. KN393/4 as well as BO1912/2-1. The work in Beijing was supported by the NSFC, the MOST (973 Projects No. 2011CBA00100), and CAS project (Project ITSNEM). We thank A. N. Yaresko for useful discussions.

1) See, e.g., V. I. Belyavsky and Yu. V. Kopaev: Phys. Rev. B **67** (2003) 024513; T. Dahm *et al.*: Nat. Phys. **5** (2009) 217, and references therein.
2) S. Raghu *et al.*: Phys. Rev. B **77** (2008) 220503(R).
3) D. J. Singh: Phys. Rev. B **78** (2008) 094511.
4) I. A. Nekrasov *et al.*: JETP Lett. **88** (2008) 155.
5) V. B. Zabolotnyy *et al.*: Nature (London) **457** (2009) 569.
6) D. Hsieh *et al.*: arXiv:0812.2289.
7) H. Liu *et al.*: Phys. Rev. Lett. **105** (2010) 027001.
8) T. Sato *et al.*: Phys. Rev. Lett. **103** (2009) 047002.
9) V. B. Zabolotnyy *et al.*: Physica C **469** (2009) 448.
10) D. H. Lu *et al.*: Nature (London) **455** (2008) 81.
11) A. I. Coldea *et al.*: Phys. Rev. Lett. **101** (2008) 216402.
12) H. Ding *et al.*: Europhys. Lett. **83** (2008) 47001.
13) C. Liu *et al.*: Phys. Rev. Lett. **101** (2008) 177005.
14) H. Luo *et al.*: Supercond. Sci. Technol. **21** (2008) 125014.
15) G. L. Sun *et al.*: arXiv:0901.2728.
16) J. T. Park *et al.*: Phys. Rev. Lett. **102** (2009) 117006.
17) The details of setup geometry can be found in D. S. Inosov *et al.*: Phys. Rev. B **77** (2008) 212504.
18) In investigation of three-dimensionality of iron pnictides ARPES studies concentrate on the undoped and electron-doped samples [W. Malaeb *et al.*: J. Phys. Soc. Jpn. **78** (2009) 123706; T. Kondo *et al.*: Phys. Rev. B **81** (2010) 060507(R)]. From $Ba_{1-x}K_xFe_2As_2$ ARPES data taken with different excitation energies (partially published in ref. 22) we can estimate the upper limit for k_z-dispersion — the variation of the sizes for Γ-barrels is not more than ±15%. The computation of the in-plane electrical transport, which assumes the electronic structure to be two-dimensional with the parameters, corresponding to the k_z-averaged ones of the real three-dimensional structure, should provide fairly good accuracy in our case.
19) D. V. Evtushinsky *et al.*: Phys. Rev. Lett. **100** (2008) 236402.
20) The expression for $\delta\sigma_{xx}$ is consistent with J. M. Harris *et al.*: Phys. Rev. Lett. **75** (1995) 1391; N. E. Hussey: Eur. Phys. J. B **31** (2003) 495, although rewritten in a form more convenient for the present consideration.
21) In terms of band dispersion, $\varepsilon(\mathbf{k})$, Fermi velocity and FS curvature read $v_F \equiv |\nabla\varepsilon|/\hbar$, $1/\rho_F \equiv \nabla^2\varepsilon \cdot |\nabla\varepsilon| - (\nabla|\nabla\varepsilon|, \nabla\varepsilon)/(\nabla\varepsilon, \nabla\varepsilon)$.
22) D. V. Evtushinsky *et al.*: New J. Phys. **11** (2009) 055069.
23) The actual value is given for a simple model with two hole-like and two electron-like circular FS sheets with the same effective mass and the average Fermi momentum of the hole-like barrels of 0.4 $Å^{-1}$. The obtained R_H is very close to the one, resulting from the rigorously calculated band structure (A. N. Yaresko: private communication). Details of the band structure calculation are available in A. N. Yaresko *et al.*: Phys. Rev. B **79** (2009) 144421.
24) W. W. Schulz *et al.*: Phys. Rev. B **45** (1992) 10886.
25) W. W. Schulz *et al.*: Phys. Rev. B **46** (1992) 14001.
26) A. Narduzzo *et al.*: Phys. Rev. B **77** (2008) 220502(R).
27) H. Yang *et al.*: Phys. Rev. Lett. **101** (2008) 067001.
28) L. Fang *et al.*: Phys. Rev. B **80** (2009) 140508(R).
29) X. F. Wang *et al.*: New J. Phys. **11** (2009) 045003.
30) R. H. Liu *et al.*: Phys. Rev. Lett. **101** (2008) 087001.
31) Presented here considerations rely on the results, obtained in the Fermi-liquid-like approach. Though pure Fermi liquid theory is not always applicable to the electrons in solids, e.g., in the vicinity of phase transition and importance of order fluctuations (see ref. 45 and references therein), the natural extension of this transparent theory may be useful even in description of correlated systems. In particular, the band dispersion, extracted from the spectral function (measured in ARPES experiments), should well represent the effective band dispersion and Fermi surface, defining the electron dynamics.
32) D. S. Inosov *et al.*: Phys. Rev. Lett. **104** (2010) 187001.
33) A manuscript with the calculation of the LiFeAs Hall coefficient from ARPES and comparison to the magnetotransport measurements is under preparation. Measurements of the Hall effect on LiFeAs are described in O. Heyer *et al.*: arXiv:1010.2876.
34) S. V. Borisenko *et al.*: Phys. Rev. Lett. **105** (2010) 067002.
35) T. Yoshida *et al.*: arXiv:1008.2080.
36) D. V. Evtushinsky *et al.*: Phys. Rev. B **74** (2006) 172509.
37) P. Szabo *et al.*: Phys. Rev. B **79** (2009) 012503.
38) D. V. Evtushinsky *et al.*: Phys. Rev. B **79** (2009) 054517.
39) K. Hashimoto *et al.*: Phys. Rev. Lett. **102** (2009) 207001.
40) M. Yashima *et al.*: J. Phys. Soc. Jpn. **78** (2009) 103702.
41) S. Kasahara *et al.*: Phys. Rev. B **81** (2010) 184519.
42) Y. Nakai *et al.*: Phys. Rev. Lett. **105** (2010) 107003.
43) A. A. Kordyuk *et al.*: Phys. Rev. B **79** (2009) 020504(R).
44) S. V. Borisenko *et al.*: Phys. Rev. Lett. **100** (2008) 196402; S. V. Borisenko *et al.*: Phys. Rev. Lett. **102** (2009) 166402; D. S. Inosov *et al.*: Phys. Rev. B **79** (2009) 125112.
45) Y. Nakajima *et al.*: J. Phys. Soc. Jpn. **76** (2007) 024703.